Polymer Engineering & Science

WILEY | spe INSPIRING PLASTICS PROFESSIONALS

RESEARCH ARTICLE OPEN ACCESS

Enhancing Mechanical Performance of FDM-Printed ABS Parts Through Annealing Optimization

Elifnur Kösemen[1] | Mustafa Bakkal[1] | Ali Taner Kuzu[2]

[1]Department of Mechanical Engineering, Istanbul Technical University, Istanbul, Turkey | [2]Department of Mechanical Engineering, Isik University, Istanbul, Turkey

Correspondence: Ali Taner Kuzu (alitaner.kuzu@isikun.edu.tr)

Received: 17 March 2025 | **Revised:** 2 May 2025 | **Accepted:** 1 June 2025

Funding: This work was supported by the Bilimsel Araştırma Projeleri Birimi, İstanbul Teknik Üniversitesi (MGA-2020-42593).

Keywords: ABS | annealing | FDM | impact strength | tensile strength

ABSTRACT

This study examines the impact of annealing on the mechanical properties of acrylonitrile butadiene styrene (ABS) parts produced using fused deposition modeling (FDM). The research investigates how different annealing temperatures (90°C, 105°C, and 120°C), production orientations (upright, on edge, and flat), and infill patterns influence hardness, tensile strength, and impact resistance. Experiments were conducted using a Stratasys F370 printer, and samples were tested following ISO standards for mechanical performance. Results indicated that annealing at 90°C and 105°C generally improved hardness, tensile strength, and impact resistance, particularly for upright and on-edge orientations. However, annealing at 120°C led to a decrease in these properties, likely due to microstructural changes observed through scanning electron microscopy (SEM) and differential scanning calorimetry (DSC) analysis. The study highlights the importance of optimizing production parameters and annealing conditions to achieve desired mechanical properties in FDM-printed ABS parts. These findings may inform post-processing strategies for enhancing the reliability and performance of additive manufactured components, particularly for applications in industries utilizing ABS materials for customized and prototype parts.

1 | Introduction

In recent years, the expansion of research using 3D printing technology has had a tremendous impact on different industries, providing essential contributions to manufacturing processes [1]. Notably, the use of 3D printing has transformed manufacturing by allowing for the rapid manufacture of sophisticated designs, reducing production timelines for huge and complex items, and increasing overall efficiency [2]. Furthermore, the incorporation of 3D printing has expedited workflows, enabling real-time monitoring and automation in manufacturing facilities. Recent studies also highlight its growing role in biomedical applications [3], energy harvesting [4], and composite reinforcement via nanofillers [5], further demonstrating the versatility and cross-disciplinary relevance of additive manufacturing. Among the several 3D printing technologies available, fused deposition modeling (FDM) stands out, especially in the field of plastic material manufacturing. FDM is popular due to its versatility, cost-effectiveness, and accessibility, with a wide range of materials available for use, including acrylonitrile butadiene styrene (ABS), polycarbonate (PC), PC-ABS, and ASA [6, 7].

Additive manufacturing has revolutionized the production of components across industries, offering unique advantages such as design flexibility and rapid prototyping. Understanding the mechanical behaviors of additively manufactured parts is crucial for optimizing manufacturing processes and ensuring component reliability. In recent studies exploring additive manufacturing techniques, several investigations have examined the mechanical behaviors of components produced using different

Summary

- Annealing at 90°C and 105°C improves ABS properties, but 120°C reduces strength.
- SEM analysis reveals reduced voids and improved layer fusion post-annealing.
- Optimized annealing improves FDM part reliability for industrial applications.

materials and printing methodologies. Ziemian et al. [8] examined the influence of meso-structure on the tensile behavior and fatigue life of ABS components fabricated via melt deposition modeling, highlighting anisotropic characteristics and superior fatigue performance in specific orientations. Fisher and Schoppner [9] focused on the fatigue behavior of Ultem 9085 components, noting anisotropy under varying loads and the impact of chemical exposure on tensile strength. Rodríguez-Panes et al. [10] conducted a comparative analysis of PLA and ABS filament components, revealing the significant influence of FDM parameters on mechanical performance. Meanwhile, Dawoud et al. [11] investigated the mechanical behavior of ABS components produced through FDM, showcasing the importance of parameter selection for achieving comparable properties to injection-molded parts. Gorski et al. [12] explored the impact of orientation on ABS specimens' impact strength, emphasizing the role of optimal orientation in enhancing mechanical properties. Additionally, Khabia and Jain [13] examined the mechanical properties of components printed with different FDM printers and ABS filaments, highlighting the significance of printer-filament combinations in achieving desired tensile properties. Lastly, Popescu et al. [7] conducted a systematic literature review on polymer filaments, emphasizing the influence of process parameters such as layer thickness and infill width on tensile strength in FDM samples. These collective findings provide valuable insights into optimizing additive manufacturing processes for enhanced mechanical performance across various materials and printing conditions. However, even with optimized processing parameters, FDM-printed parts inherently contain internal voids and other microstructural defects that can significantly diminish their tensile strength and toughness [7–11]. To address these issues, post-processing strategies such as annealing are often employed to enhance interlayer bonding and improve overall mechanical performance.

Post-processing techniques play a crucial role in enhancing the mechanical properties of 3D-printed components, offering opportunities to improve strength, surface finish, and dimensional stability. Demircali et al. [14] investigate the effects of acetone post-processing on tensile strength, dimensional changes, and mass variation. Their results show significant enhancements in tensile strength, particularly at higher temperatures and longer exposure times, indicating the effectiveness of acetone treatment in altering the mechanical and physical properties of 3D-printed ABS parts. Following this, Seok et al. [15] delve into the mechanical properties of FDM 3D-printed carbon fiber-reinforced composites derived from ABS filaments under annealing conditions. Their study reveals that annealing improves tensile and flexural strengths by reducing voids and inter-fiber gaps, with the most notable enhancements observed in samples containing 20 wt% reinforced carbon fiber. Additionally, Torres et al. [16] investigate the optimization of annealing and vapor smoothing treatments on the surface roughness and tensile properties of FDM-printed ABS. Through comprehensive testing, they identify optimal parameters, highlighting the significant improvement in surface roughness through vapor smoothing and the superior enhancement in tensile properties with annealing at 100°C for 60 min. Moreover, Singh et al. [17] introduce a novel heat treatment method to enhance the mechanical and surface properties of FFF-printed ABS components. Utilizing Taguchi experimental design, they optimize annealing parameters to improve surface roughness, hardness, dimensional accuracy, and various mechanical strengths, thereby enhancing the overall quality of FFF parts. Butt et al. [18] explore the effects of annealing on a range of polymeric materials commonly used in FFF printing, including ABS and PLA, as well as metal-infused thermoplastics like copper-enhanced PLA and aluminum-enhanced ASA. Their comprehensive analysis reveals that while annealing significantly enhances the mechanical properties of semicrystalline materials like PLA and copper-enhanced PLA, its impact on amorphous materials like ABS and aluminum-enhanced ASA is comparatively limited. Stojković et al. [19] explored the effects of annealing parameters on PLA, PETG, and carbon fiber-reinforced PETG, revealing the significant influence of layer height on tensile strength. He et al. [20] investigated the mechanical and tribological properties of PEEK, determining optimal FDM parameters and annealing temperatures to enhance mechanical strength and reduce wear rate. Quassil et al. [21] studied the impact of printing parameters and annealing on the properties of 3D-printed PEI parts, emphasizing print speed as the most influential factor. Srinidhi et al. [22] examined the mechanical properties of PETG and CFPETG specimens, highlighting the role of infill patterns in improving mechanical properties post-heat treatment. Kumar et al. [23] explored the effect of infill density on PETG and CFPETG parts, demonstrating significant improvements in mechanical properties, particularly at higher densities. Collectively, these studies provide valuable insights into optimizing additive manufacturing processes for enhanced mechanical performance and offer guidance for producing functional parts with various materials and printing conditions.

In this study, ABS-M30 filament was used in the Stratasys F370 3D printer to produce samples. Tool paths and production parameters were determined using Insight and GrabCAD software. Hardness measurements were taken post-production, while tensile and impact tests were conducted following ISO standards. Annealing was performed at temperatures of 90°C, 105°C, and 120°C, with DSC analysis assessing thermal stability and chemical structure changes. Optical and SEM examinations provided insights into microstructural alterations induced by annealing.

2 | Materials and Methods

The production of samples involved using ABS-M30 filament in the Stratasys F370 3D printer. Insight and GrabCAD software were utilized to slice the geometry and determine the tool paths and production parameters. Firstly, the necessary parameters for production were processed using the Insight software, followed by slicing. Subsequently, the supports and tool paths were created based on the combinations of production parameters

outlined in Table 1. Notably, all combinations exhibited visible raster spacing of 0.018 mm, inner raster spacing of 0.022 mm, internal raster air gap of 0.001 mm, and a layer height of 0.1778 mm. An illustrative example of the tool paths is provided in Figure 1.

The hardness measurements were conducted on the specimens after production for each combination of production parameters. A Shore hardness tester was preferred because it provides a rapid, standardized, and nondestructive method of evaluating surface hardness. It allows accurate assessment of thermoplastic materials like ABS directly on the printed parts without additional sample preparation, ensuring robust and reliable comparison across production parameters. Measurements were taken from three different points on the surface, and the average value was determined as the hardness value.

Tensile strength and strain at fracture were determined by tensile test. The tests were carried out in three repetitions for each production parameter, using a Shimadzu 50 kN tensile tester with a tensile speed of 2 mm/min following the requirements of the standard. The dimensions of the tensile test specimen, produced according to the ISO 527 standard, are given in Figure 2a. The production of tensile test specimens was carried out using two different orientations: upright and on edge. Impact test specimens were produced in two different orientations, flat and on edge. The impact test specimen dimensions in accordance with the ISO 180 standard produced are given in Figure 2b, and the impact test was performed using the Charpy impact tester. Figure 2c presents the print directions of the tensile and impact test specimens.

To investigate the impact of annealing on the mechanical strength of ABS materials with a reference glass transition temperature of 105°C, three different annealing temperatures were selected: 90°C, 105°C, and 120°C. Two different

TABLE 1 | Production parameters.

Infill pattern	Sparse high density (SPH) and hexagram (HXG)
Orientation	On edge, upright, and flat
Contour number	1 and 2

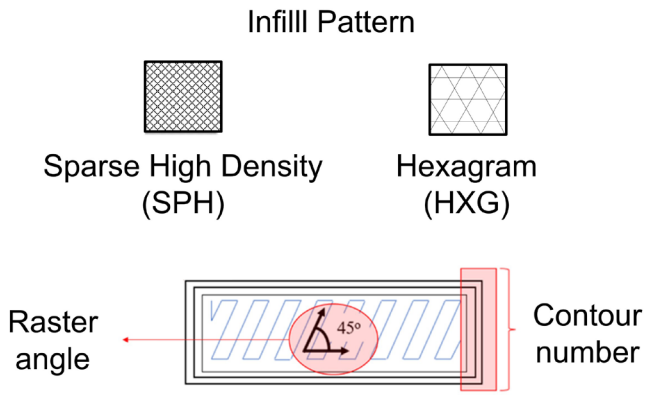

FIGURE 1 | Example of the created tool paths.

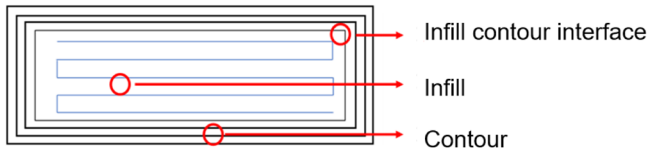

FIGURE 3 | SEM investigation regions.

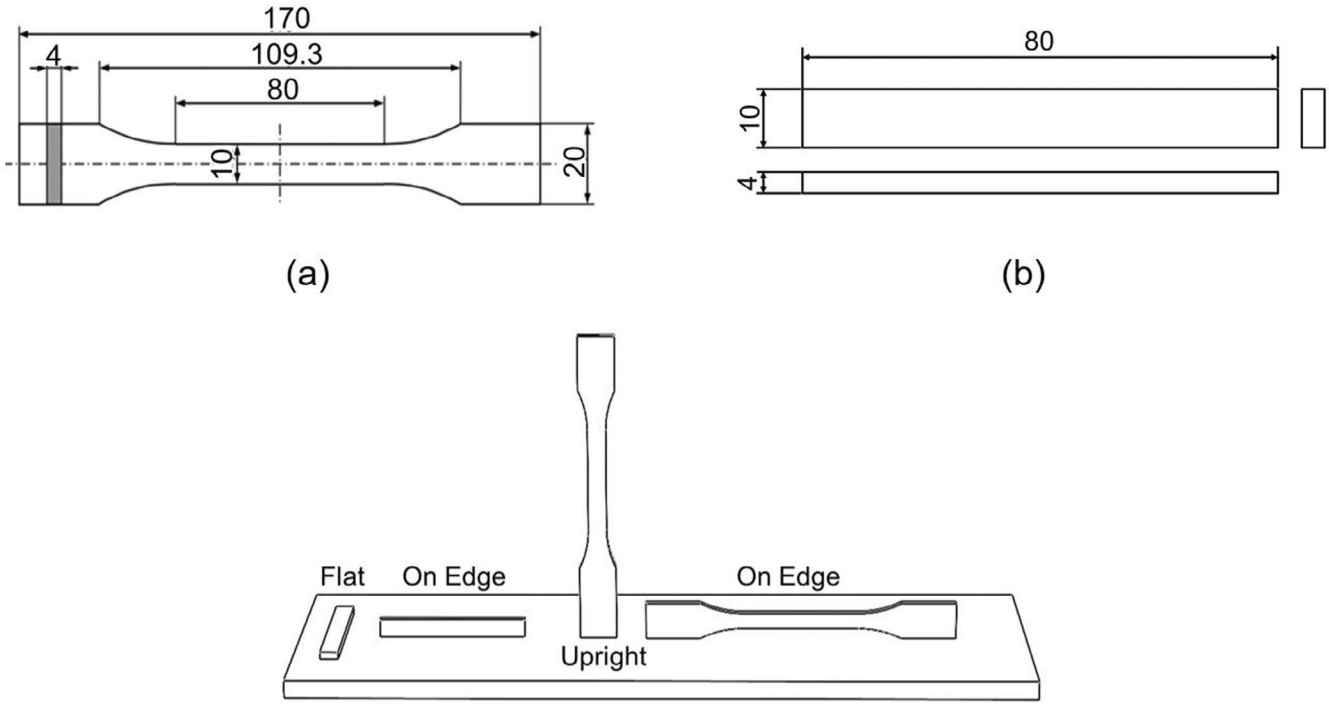

FIGURE 2 | The geometry of the (a) tensile test specimen, (b) the impact test specimen, and (c) print orientations.

annealing times, 15 and 30 min, were tested for each temperature. It was observed that 30-min annealing caused significant deformation and dimensional instability in the printed parts.

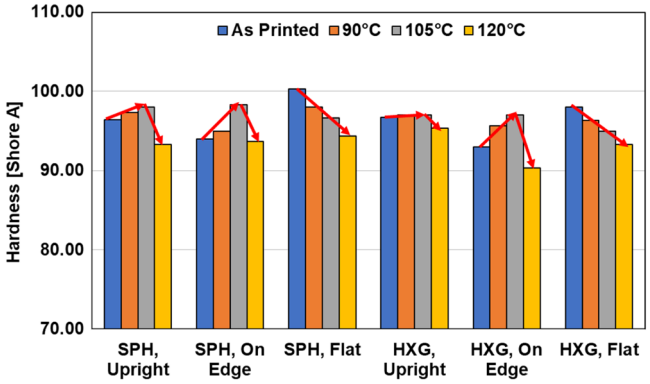

FIGURE 4 | Hardness of specimen produced by SPH and HXG infill pattern.

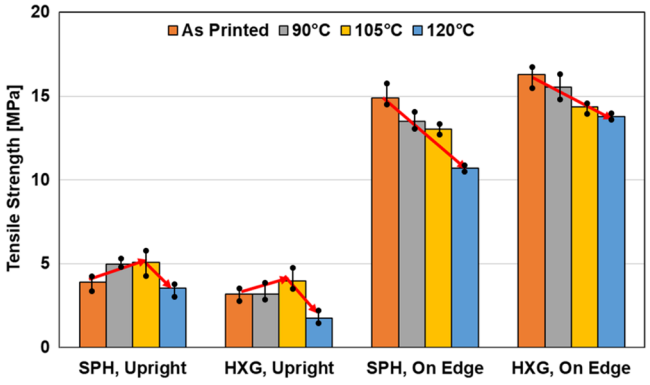

FIGURE 5 | The tensile strengths of specimens produced by SPH and HXG infill parameters.

Thus, 15 min was finalized as the optimal annealing time as it effectively enhanced mechanical properties without compromising part geometry, balancing strength improvement and shape preservation. Therefore, the experiment will proceed with annealing at the selected temperatures for a duration of 15 min to assess any changes in mechanical strength.

To investigate the thermal stability and potential changes in the chemical structure of ABS samples annealed at three different temperatures, differential scanning calorimetry (DSC) analysis was conducted. The DSC analysis aimed to analyze the glass transition temperature and specific heat of the samples and was performed on a SETARAM DSC 131 device with 10°C increments, up to 300°C.

The microstructure of annealed samples was first examined using an optical microscope. To further analyze the effects of annealing, the fracture surfaces of the samples were investigated using a scanning electron microscope (SEM). The PhenomWorld—Phenom XL model SEM device was utilized to capture images of the samples from various regions, including between the contour, infill, and infill raster interface of the tensile and impact specimen, given in Figure 3. These SEM images provide further insight into the microstructural changes induced by annealing and will be presented in this paper.

3 | Results and Discussion

Figure 4 shows the effect of annealing on the surface hardness of printed ABS specimens regarding orientation. It is observed that annealing temperatures of 90°C and 105°C increase the hardness of samples produced with upright and on-edge printing orientations. However, when the annealing temperature is raised to 120°C, the hardness decreases below the hardness measurements of samples without annealing. Conversely, for

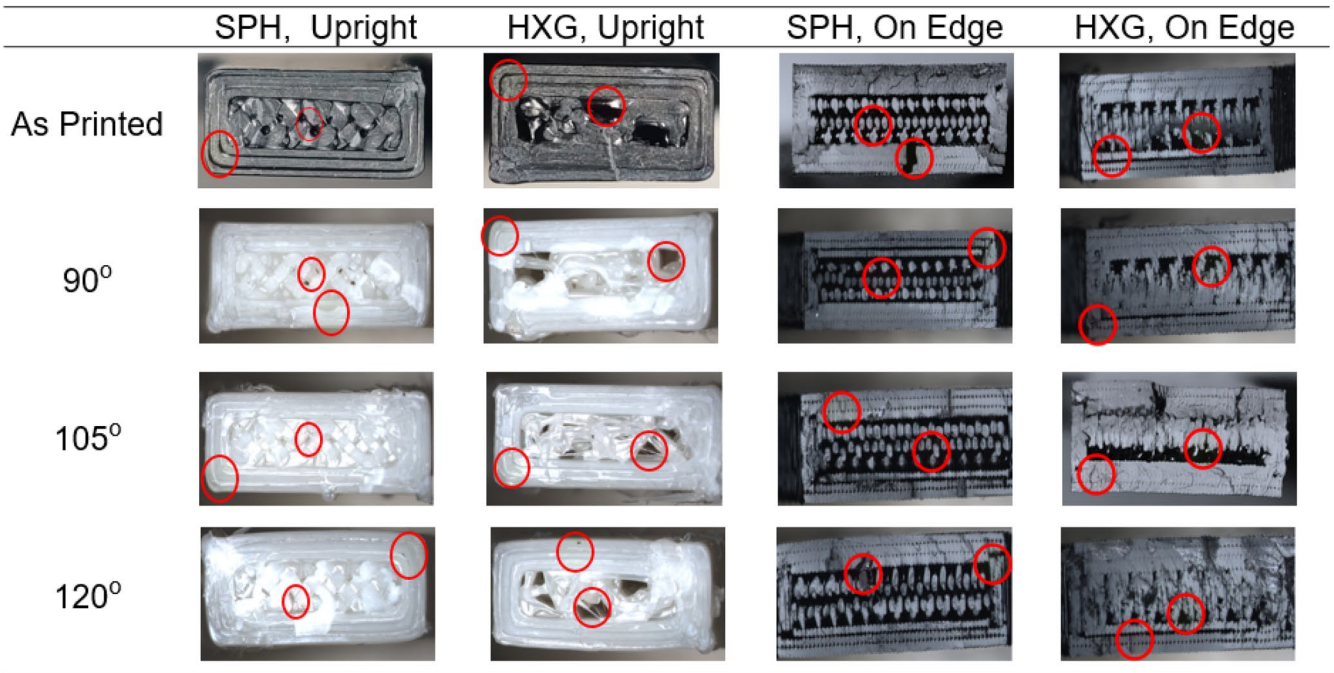

FIGURE 6 | The fracture surface micrographs of the tensile test specimen.

samples produced with the flat printing orientation, an increase in annealing temperature results in a decrease in hardness measurements.

Figure 5 shows the tensile strengths of annealed samples at various annealing temperatures, divided by production parameters. Upon analysis, different trends appear. Initially, for samples printed with the SPH infill pattern in the upright orientation, there is a steady increase in tensile strength with increasing annealing temperature, peaking at 105°C before decreasing slightly at 120°C. In contrast, samples using the HXG infill pattern in the upright position show a different trend. They show a small rise in tensile strength between 90°C and 105°C, followed by a considerable reduction at 120°C. Annealing affects SPH and HXG infills differently due to their structure. SPH's dense, continuous pattern allows better polymer flow and bonding, improving strength at 90°C and 105°C. HXG's honeycomb geometry limits flow and creates stress points, causing weaker improvement and a sharper drop at 120°C. Furthermore, when comparing samples printed upright versus on edge, it is clear that the on-edge orientation produces greater tensile strengths across all annealing temperatures and infill patterns. This shows that the printed part's orientation during production significantly impacts its mechanical properties after annealing. These findings highlight

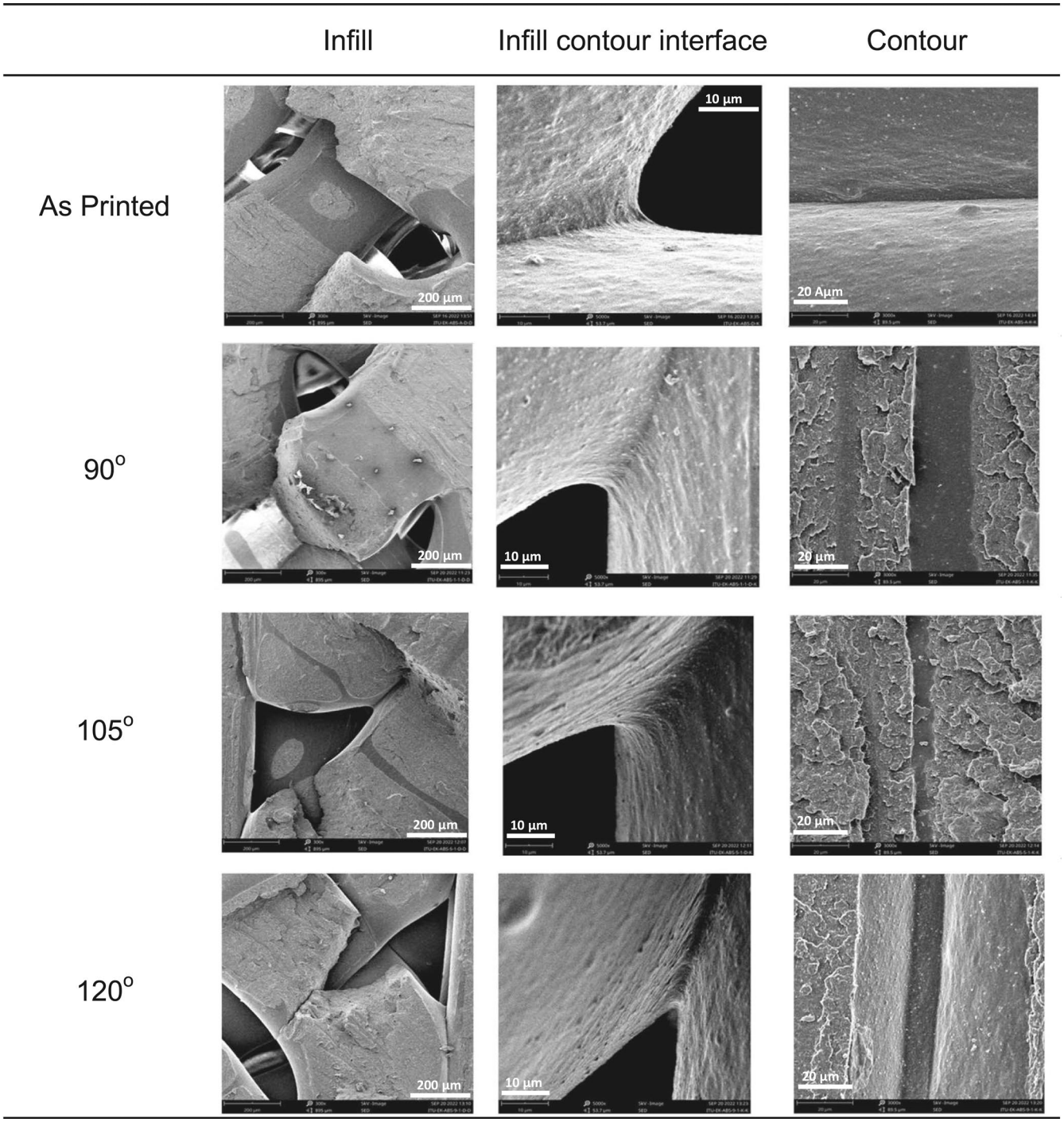

FIGURE 7 | The SEM images of the tensile test specimen produced by the SPH infill pattern and upright orientation.

the need to adjust both the annealing temperature and the production parameters to achieve the optimum mechanical performance in FDM-produced plastic components.

The samples that were annealed for 15 min at 90°C, 105°C, and 120°C, as well as those that were not annealed, were examined under an optical microscope to investigate the fracture surfaces resulting from tensile testing, as shown in Figure 6. Among the two parameter combinations in the upright orientation for both SPH and HXG infill patterns, the samples with the highest void density in the infill and between contours were those that had not been annealed. Samples annealed at 90°C showed reduced voids and separations because annealing below the glass transition temperature promotes filament diffusion without excessive softening, resulting in stronger interlayer bonding and reduced microvoids. At 105°C, voids and separations were almost nonexistent, with filaments filling the interstitial spaces. However, at 120°C, indications of contour separation and light void development reappeared. It was observed that the tensile strength increased with annealing temperatures of 90°C and 105°C across all production parameter combinations, but decreased at 120°C. Given that the glass transition temperature of ABS material

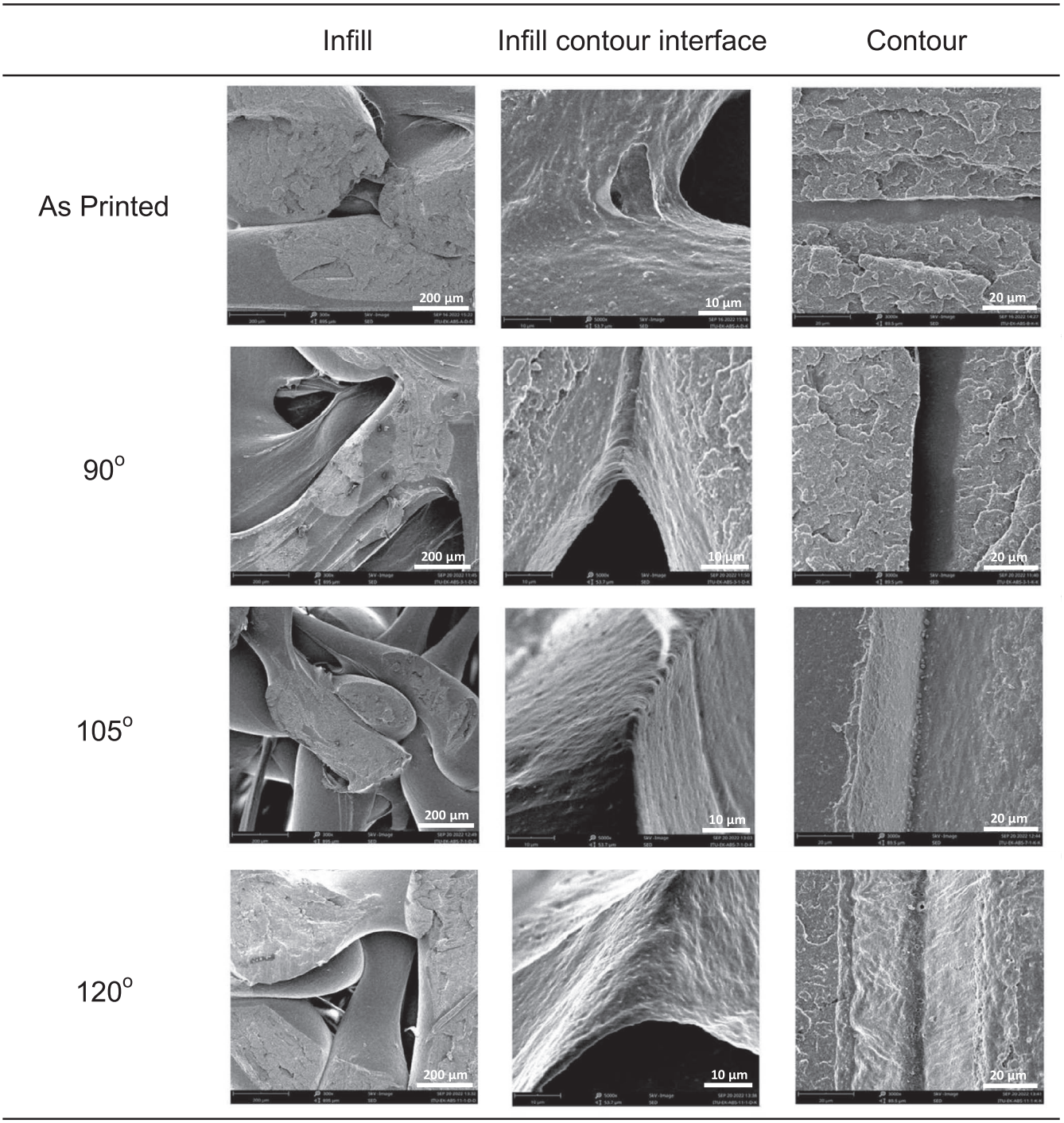

FIGURE 8 | The SEM images of tensile test specimen produced by HXG infill pattern and upright orientation.

is 105°C, annealing above this temperature led to disruptions within the internal layers of the material, triggering notch effects and resulting in a decrease in tensile strength.

Furthermore, when examining the damaged surfaces after tensile testing in the on-edge orientation for both SPH and HXG infill patterns, it was noted that an increase in annealing temperature beyond T_g (105°C) did not uniformly reduce void structure but instead introduced new voids and cracks. Excessive thermal energy at 120°C led to material softening, nonuniform internal stress relaxation, and structural instability, counteracting the benefits observed at lower temperatures.

The SEM images of fracture surfaces from tensile tests conducted after annealing are presented in Figure 7 for the SPH infill pattern and in Figure 8 for the HXG infill parameter. SEM analysis focused on examining the infill, infill–contour interface, and contour regions of the samples, with their locations indicated in Figure 4.

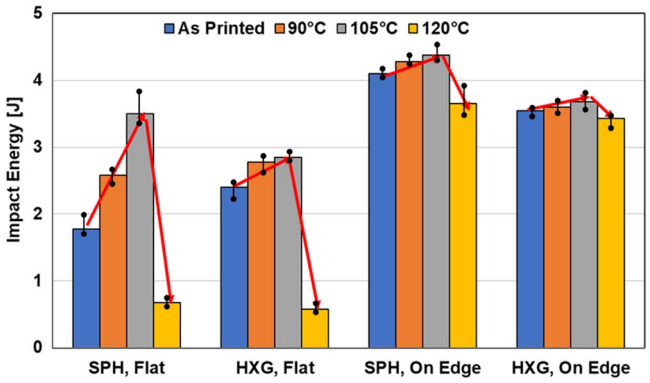

FIGURE 9 | The impact energy of the specimen produced with SPH and HXG infill parameters.

Observations from the SEM analysis revealed that samples annealed at 90°C exhibited a reduction in voids within the infill region for both infill patterns. An increase in diffusion between the infill and contour regions was also observed following annealing. However, with increasing annealing temperature, especially at 120°C, porous structure formation increased, particularly in the contour region due to thermal expansion mismatches and gravity-induced deformation, resulting in separation at contour–infill interfaces.

For samples annealed at 105°C, an increase in voids within the infill region compared to those annealed at 90°C was observed, accompanied by the formation of cracks within the infill layer. At 120°C, a distinct separation within the infill region was observed. While an increase in diffusion between the infill and contour regions was observed at 105°C, at 120°C, this diffusion line sharpened again, making separation more likely.

Irrespective of the infill pattern used in upright production, without annealing, the tensile strength decreased sequentially with annealing temperatures of 90°C, 105°C, and 120°C, respectively. It was noted that the primary reason for this decrease was the porous structure in the contour region, supported by crack and void mechanisms within the internal structure.

Figure 9 shows the impact energy of annealed samples at different annealing temperatures and production conditions. For both SPH and HXG infill patterns, there is a general tendency of increased impact energy as annealing temperatures rise to the glass transition temperature of 105°C. This indicates that annealing at higher temperatures can improve the impact resistance of printed samples. However, annealing above the glass transition temperature results in decreased impact energy showing that excessive annealing may reduce impact resistance. When comparing the impact energy of SPH and HXG infill

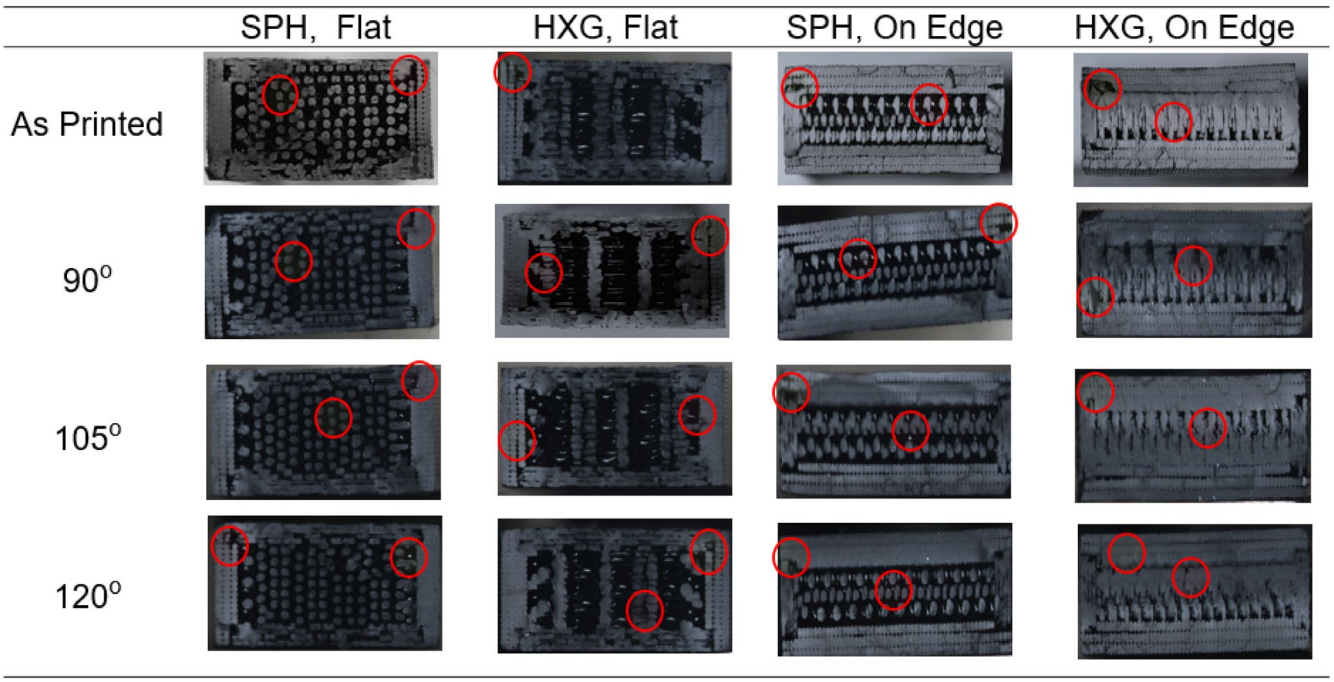

FIGURE 10 | The fracture surface micrographs of tensile test specimen.

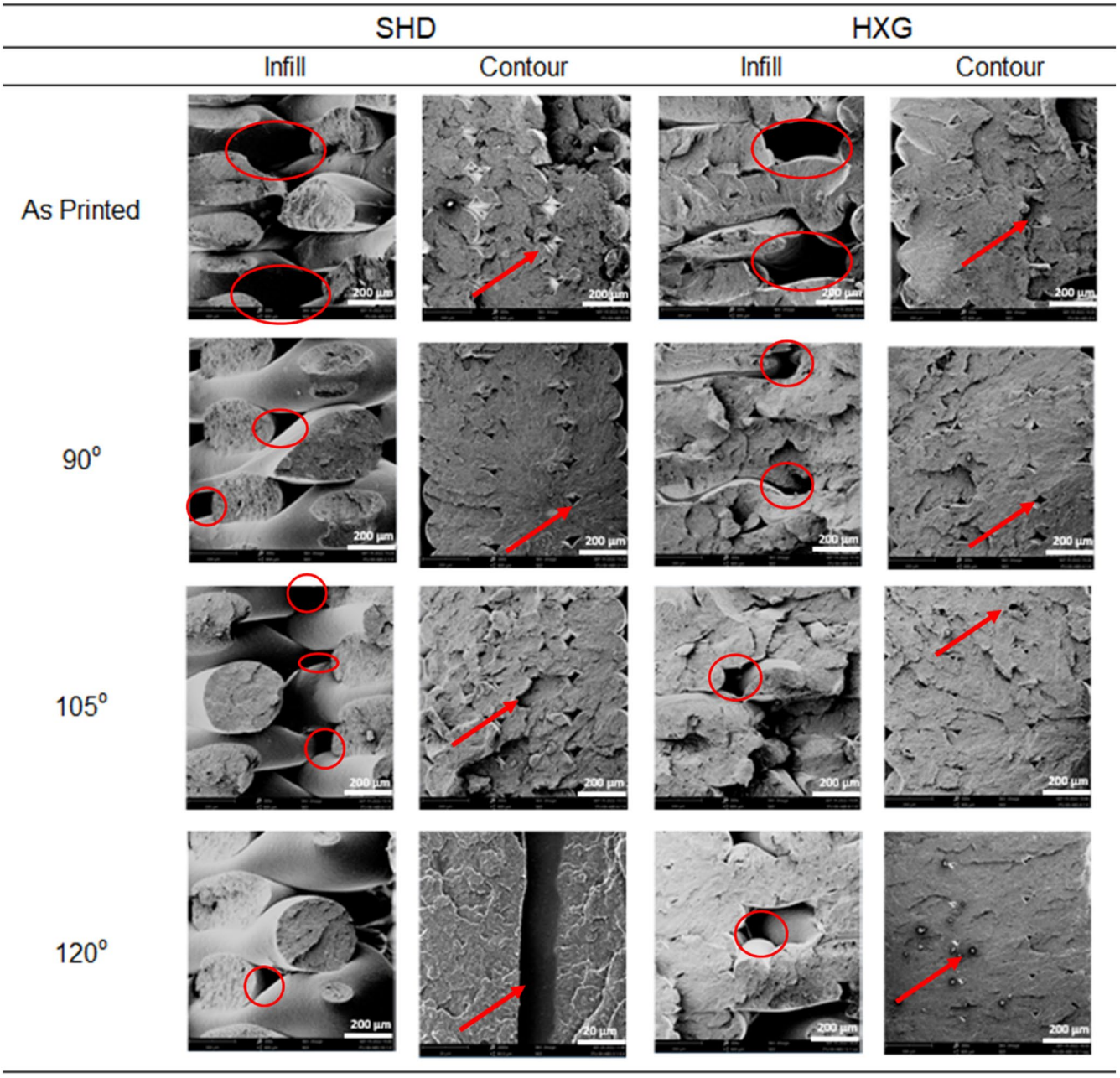

FIGURE 11 | The SEM images of the impact test specimen produced by SPH and HXG infill patterns.

patterns, it appears that there are differences in impact resistance. At certain annealing temperatures, one infill pattern may have more impact energy than another.

Samples printed on the edge consistently have higher impact energy than those printed flat, regardless of the infill pattern or annealing temperature. This shows that the orientation of the printed item during production has a major effect on its impact resistance, with on-edge printing typically resulting in better performance.

Figure 10 displays surface images of impact test fractures for annealed samples at different annealing temperatures and production conditions. In samples annealed at 90°C, the formation of bonds between internal structure layers and contours was observed, with these bonds becoming more pronounced in samples annealed at 105°C. However, in samples annealed at 120°C, an increase in cracks and voids was observed within the internal structure and between contours. Regardless of the production orientation and flat production direction, an increase in impact strength was observed with annealing at 90°C and 105°C across all production parameter combinations. Conversely, the application of an annealing temperature of 120°C led to a decrease in impact strength. This decrease is attributed to the fact that annealing above the glass transition temperature of ABS material, which is 105°C, results in a decrease in impact strength. Although the notch effect decreases with increasing annealing temperature, it is believed that the microcracks formed within the material's internal structure above 120°C activate a brittle behavior mechanism.

The SEM images of fracture surfaces from impact tests conducted after annealing are presented in Figure 11 for the SPH

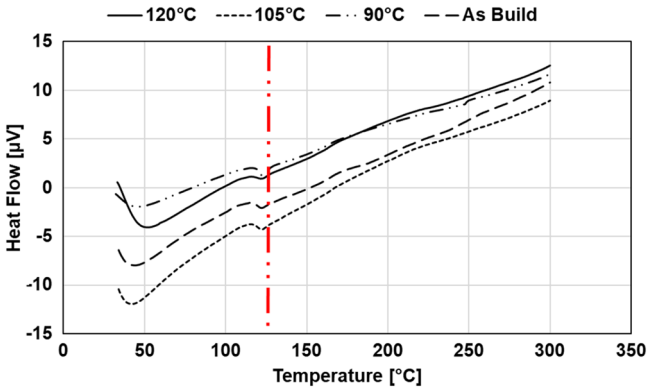

FIGURE 12 | DSC analysis of graphs of the annealed samples and ABS M-30 filament.

and in the hexagram HXG infill pattern. In samples subjected to impact tests, SEM analysis revealed that, irrespective of the orientation and infill pattern, samples annealed at 90°C exhibited a reduction in voids within the infill region and an increase in diffusion between layers in the contour region.

Furthermore, in samples annealed at 105°C and 120°C, the amount of diffusion in the contour region increased proportionally with temperature. At 120°C, it was observed that fusion of internal fillings resulted in larger internal structure voids. Despite the increased layer diffusion in the contour region, it is believed that the formation of these voids within the internal structure at 120°C reduces impact strength.

Across all production orientations and without annealing, an increase in impact strength was observed at annealing temperatures of 90°C and 105°C. However, a decrease in impact strength was observed at 120°C annealing, suggesting that the void formation within the internal fillings supports changes in strength.

In Figure 12, DSC analysis graphs of the samples applied 90°C, 105°C, and 120°C annealing are shown. The results of the DSC analysis on the filament are in agreement with the DSC analyses for ABS material in the literature. When the DSC analyses of the annealed samples were examined, it was determined that there was no major difference in the glass transition temperatures.

4 | Conclusions

This study investigated the effects of annealing temperature, printing orientation, and infill pattern on the mechanical performance of FDM-printed ABS parts. The key findings can be summarized as follows:

Annealing at 105°C for 15 min significantly enhanced mechanical properties without compromising dimensional stability. At this temperature, tensile strength increased by up to 25%, impact energy by 15%–20%, and surface hardness by 2–4 Shore A units compared to unannealed samples.

The SPH infill pattern consistently outperformed the HXG pattern in mechanical performance. SPH samples exhibited 5%–10% higher tensile strength and demonstrated greater structural integrity after annealing, particularly at elevated temperatures. This was attributed to the more uniform internal structure and reduced stress concentrations in SPH infill.

Samples printed in the on-edge orientation achieved the highest mechanical strength, with maximum tensile strength reaching ~35 MPa in SPH-filled samples after 105°C annealing. In contrast, upright-printed samples showed the most significant relative improvements after annealing, though they remained mechanically inferior to on-edge specimens.

Exceeding the glass transition temperature of ABS led to adverse effects, including the formation of internal voids, microcracks, and contour–infill separations. These structural defects caused tensile strength and impact resistance to decline by 10%–15% and surface hardness to drop below initial values.

SEM analysis revealed that annealing at 90°C–105°C promoted filament diffusion and interlayer bonding, thereby reducing voids. Conversely, 120°C annealing caused void coalescence and crack initiation, explaining the deterioration in mechanical performance. DSC analysis confirmed that thermal changes did not alter the glass transition temperature, reinforcing that observed effects were structural rather than thermal-chemical.

In conclusion, the combination of SPH infill, on-edge printing orientation, and annealing at 105°C for 15 min provides an effective strategy to optimize the mechanical properties of FDM-printed ABS parts. These findings offer practical guidelines for manufacturers seeking to enhance part strength and reliability in functional and industrial applications.

Author Contributions

Elifnur Kösemen: experimentation, investigation, data curation. **Mustafa Bakkal:** supervision, conceptualization, writing – review and editing. **Ali Taner Kuzu:** supervision, conceptualization, visualization, writing – review and editing.

Acknowledgments

The authors would like to acknowledge the support and resources provided by Ford Otosan Factory and Istanbul Technical University for this study. This research was supported by the Scientific Research Projects Unit (BAP) of Istanbul Technical University under Project Code MGA-2020-42593.

Conflicts of Interest

The authors declare no conflicts of interest.

Data Availability Statement

The data that support the findings of this study are available from the corresponding author upon reasonable request.

References

1. B. Lu, D. Li, and X. Tian, "Development Trends in Additive Manufacturing and 3D Printing," *Engineering* 1 (2015): 85–89, https://doi.org/10.15302/J-ENG-2015012.

2. I. J. Petrick and T. W. Simpson, "3D Printing Disrupts Manufacturing: How Economies of One Create New Rules of Competition,"

Research-Technology Management 56 (2013): 12–16, https://doi.org/10.5437/08956308X5606193.

3. S. Talib, S. Gupta, V. Chaudhary, P. Gupta, and M. A. Wahid, "Additive Manufacturing: Materials, Techniques and Biomedical Applications," *Materials Today Proceedings* 1, no. 46 (2021): 6847–6851, https://doi.org/10.1016/j.matpr.2021.04.438.

4. A. S. Lemine, J. Bhadra, K. K. Sadasivuni, et al., "3D Printing Flexible Ga-Doped ZnO Films for Wearable Energy Harvesting: Thermoelectric and Piezoelectric Nanogenerators," *Journal of Materials Science: Materials in Electronics* 35, no. 24 (2024): 1639, https://doi.org/10.1007/s10854-024-13372-z.

5. J. S. Krishna, V. Chaudhary, J. Mehta, P. Malhotra, S. Gupta, and P. Gupta, "Synergistic Reinforcement of Nanofillers in Biocomposites Developed by Additive Manufacturing Techniques," *Biomass Conversion and Biorefinery* 14, no. 13 (2024): 13691–13706, https://doi.org/10.1007/s13399-022-03395-z.

6. K. V. Wong and A. Hernandez, "A Review of Additive Manufacturing," *International Scholarly Research Notices* 2012 (2012): 208760, https://doi.org/10.5402/2012/208760.

7. D. Popescu, A. Zapciu, C. Amza, F. Baciu, and R. Marinescu, "FDM Process Parameters Influence Over the Mechanical Properties of Polymer Specimens: A Review," *Polymer Testing* 69 (2018): 157–166, https://doi.org/10.1016/j.polymertesting.2018.05.004.

8. S. Ziemian, M. Okwara, and C. W. Ziemian, "Tensile and Fatigue Behavior of Layered Acrylonitrile Butadiene Styrene," *Rapid Prototyping Journal* 21, no. 3 (2015): 270–278, https://doi.org/10.1108/rpj-09-2013-0086.

9. M. Fischer and V. Schöppner, "Fatigue Behavior of FDM Parts Manufactured With Ultem 9085," *JOM* 69 (2017): 563–568, https://doi.org/10.1007/s11837-016-2197-2.

10. A. Rodríguez-Panes, J. Claver, and A. M. Camacho, "The Influence of Manufacturing Parameters on the Mechanical Behaviour of PLA and ABS Pieces Manufactured by FDM: A Comparative Analysis," *Materials* 11, no. 8 (2018): 1333, https://doi.org/10.3390/ma11081333.

11. M. Dawoud, I. Taha, and S. J. Ebeid, "Mechanical Behaviour of ABS: An Experimental Study Using FDM and Injection Moulding Techniques," *Journal of Manufacturing Processes* 21 (2016): 39–45, https://doi.org/10.1016/j.jmapro.2015.11.002.

12. F. I. Górski, W. I. Kuczko, and R. A. Wichniarek, "Impact Strength of ABS Parts Manufactured Using Fused Deposition Modeling Technology," *Archives of Mechanical Technology and Automation* 34 (2014): 3–12.

13. S. Khabia and K. K. Jain, "Comparison of Mechanical Properties of Components 3D Printed From Different Brand ABS Filament on Different FDM Printers," *Materials Today Proceedings* 26 (2020): 2907–2914, https://doi.org/10.1016/j.matpr.2020.02.600.

14. A. A. Demircali, D. Yilmaz, A. Yilmaz, O. Keskin, M. Keshavarz, and H. Uvet, "Enhancing Mechanical Properties and Surface Quality of FDM-Printed ABS: A Comprehensive Study on Cold Acetone Vapor Treatment," *International Journal of Advanced Manufacturing Technology* 130, no. 7-8 (2024): 4027–4039, https://doi.org/10.1007/s00170-023-12929-2.

15. W. Seok, E. Jeon, and Y. Kim, "Effects of Annealing for Strength Enhancement of FDM 3D-Printed ABS Reinforced With Recycled Carbon Fiber," *Polymers* 15 (2023): 3110, https://doi.org/10.3390/polym15143110.

16. J. Torres, E. Abo, and A. J. Sugar, "Effects of Annealing and Acetone Vapor Smoothing on the Tensile Properties and Surface Roughness of FDM Printed ABS Components," *Rapid Prototyping Journal* 29 (2023): 921–934, https://doi.org/10.1108/RPJ-03-2022-0088.

17. S. Singh, M. Singh, C. Prakash, M. K. Gupta, M. Mia, and R. Singh, "Optimization and Reliability Analysis to Improve Surface Quality and Mechanical Characteristics of Heat-Treated Fused Filament Fabricated Parts," *International Journal of Advanced Manufacturing Technology* 102 (2019): 1521–1536, https://doi.org/10.1007/s00170-018-03276-8.

18. J. Butt and R. Bhaskar, "Investigating the Effects of Annealing on the Mechanical Properties of FFF-Printed Thermoplastics," *Journal of Manufacturing and Materials Processing* 4, no. 38 (2020): 10, https://doi.org/10.3390/jmmp4020038.

19. J. R. Stojković, R. Turudija, N. Vitković, et al., "An Experimental Study on the Impact of Layer Height and Annealing Parameters on the Tensile Strength and Dimensional Accuracy of FDM 3D Printed Parts," *Materials* 16, no. 13 (2023): 4574, https://doi.org/10.3390/ma16134574.

20. Y. He, M. Shen, Q. Wang, T. Wang, and X. Pei, "Effects of FDM Parameters and Annealing on the Mechanical and Tribological Properties of PEEK," *Composite Structures* 313 (2023): 116901, https://doi.org/10.1016/j.compstruct.2023.116901.

21. S. E. Ouassil, A. El Magri, H. R. Vanaei, and S. Vaudreuil, "Investigating the Effect of Printing Conditions and Annealing on the Porosity and Tensile Behavior of 3D-Printed Polyetherimide Material in *Z*-Direction," *Journal of Applied Polymer Science* 140, no. 4 (2023): e53353, https://doi.org/10.1002/app.53353.

22. M. S. Srinidhi, R. Soundararajan, K. S. Satishkumar, and S. Suresh, "Enhancing the FDM Infill Pattern Outcomes of Mechanical Behavior for As-Built and Annealed PETG and CFPETG Composites Parts," *Materials Today Proceedings* 45 (2021): 7208–7212, https://doi.org/10.1016/j.matpr.2021.02.417.

23. Y. Zhao, K. Zhao, Y. Li, and F. Chen, "Mechanical Characterization of Biocompatible PEEK by FDM," *Journal of Manufacturing Processes* 56 (2020): 28–42, https://doi.org/10.1016/j.jmapro.2020.04.063.